

Canonical Mean Filter for Almost Zero-Shot Multi-Task classification

Yong Li, Heng Wang, Xiang Ye*

Beijing University of Posts and Telecommunications

Abstract

The support set is a key to provide conditional prior for fast adaption of model in few-shot tasks. But the strict form of support set makes its construction actually difficult in practical application. Motivated by ANIL, we rethink the role of adaption in the feature extractor of CNAPs, which is a state-of-the-art representative few-shot method. To investigate the role, Almost Zero-Shot (AZS) task is designed by fixing the support set to replace the common scheme, which provides corresponding support sets for the different conditional prior of different tasks. The AZS experiment results infer that the adaptation works little in the feature extractor. However, CNAPs cannot be robust to randomly selected support sets and perform poorly on some datasets of Meta-Dataset because of its scattered mean embeddings responded by the simple mean operator. To enhance the robustness of CNAPs, Canonical Mean Filter (CMF) module is proposed to make the mean embeddings intensive and stable in feature space by mapping the support sets into a canonical form. CMFs make CNAPs robust to any fixed support sets even if they are random matrices. This attribution makes CNAPs be able to remove the mean encoder and the parameter adaptation network at the test stage, while CNAP-CMF on AZS tasks keeps the performance with one-shot tasks. It leads to a big parameter reduction. Precisely, 40.48% parameters are dropped at the test stage. Also, CNAP-CMF outperforms CNAPs in one-shot tasks because it addresses inner-task unstable performance prob-

*Corresponding author

Email address: yli@bupt.edu.cn (Xiang Ye)

lems. Classification performance, visualized and clustering results verify that CMFs make CNAPs better and simpler.

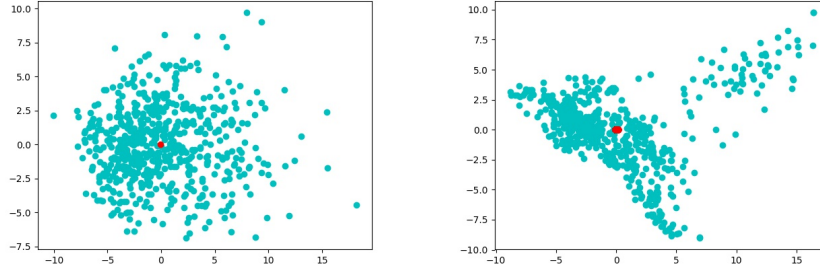
Keywords: adaptation, feature reuse, support set

1. Introduction

A critical step in few-shot learning is to conduct the adaptation with the prior information provided by the support sets [1]. Ideally, a support set ought to contain some samples with their corresponding labels for each category [1]. Existing works often construct a support set for every particular task which deals with only a limited and known number of categories. In real few-shot applications however, it is almost impossible to construct a proper support set for the whole test dataset due to the unknown number of object categories and their labels in it. Since the prior information provided by an improper support set may misguide the adaptation, this work examines the role of the feature adaptation and the generalization ability of the trained model when proper support sets are unavailable.

In literature, meta-learning methods mainly include two categories, the optimization-based and the metric-based methods. For optimization-based MAML (Model-agnostic Meta-learning) [2], ANIL (Almost No Inner Loop) [3] is proposed to investigate the role of the adaptation of feature extractor by stopping the inner loop of MAML at the test stage. ANIL finds that the feature adaptation contributed much less than the feature reuse in the generalization ability of MAML-based models. Motivated by ANIL, this work studies the role of the adaptation of feature extractor in metric-based few-shot methods. Among the metric-based methods are the representative CNAPs [4]. CNAPs are evaluated on a large-scale and complex dataset containing 10 cross-domain common datasets while other metric-based methods mainly focus on in-domain transfer ability. Since the good transfer ability of CNAPs, this work employs them to study the contribution of the feature adaptation and feature reuse.

Following the methodology of ANIL, this paper designs two ‘Almost Zero-



(a) Clustering results when the model is trained on Omniglot (b) Clustering when the model is trained on Meta-Dataset

Figure 1: The clustering results of the extracted mean features on Omniglot test images.

Shot’ (AZS) experiments, AZS-I and AZS-II, to analyze the role of feature adaptation in CNAPs. The test Meta-Dataset [5] containing 10 sub-datasets is employed. In AZS-I, one single random but fixed support set is chosen from each sub-dataset for all tasks in it to stop the adaptation, Only slight performance drop was observed.

In AZS-II, a single random but fixed support set is chosen from a particular sub-dataset but is used across all sub-datasets to further stop all the adaptation for CNAPs at the inference stage. Again, only slight performance drop is observed on seven sub-datasets (see Table 2) when the fixed support set is randomly selected from ImageNet. This observation coincides with [3] in that task-specific support sets are not necessitated for the feature extractors of few-shot learning methods. However, a dramatic performance drops was observed on few sub-datasets: Omniglot [6], Quick Draw, and Aircraft sub-datasets. Thus, a question arises: are the task-specific support sets still necessary for multi-dataset few-shot learning or the feature extractor of CNAPs relies too much on the support sets?

By deeply analyzing CNAPs, we find that the feature extractor is over-sensitive to the input support set, i.e., a small change of the support set may cause a dramatic adaptation shift when guiding the inference model. Fig. 1

shows an example of scattered mean features of corresponding support sets for different tasks. Consequently, a support set taken from a particular sub-dataset may perform poor across sub-datasets.

To address the over-sensitivity, this work proposed a dynamic-kernel-like module, Canonical Mean Filter (CMF)¹. CMF firstly applies a designed attention module to generate a vector for each sample, and then fuses the attention vectors over all image samples belonging to a support set. Then the fused vector serving as the set of weights are assigned to the kernel in next layer. In CMF, the kernels are able to map varying samples to a canonical form and become less sensitive to the input samples, so the mean prior provided by CMF is stable even when the support sets are randomly generated. Fig. 1(a) and 1(b) show the intensive and stable mean features (red points) extracted by CMF.

Similar to ANIL [3], the proposed CMF provides a better feature reuse. To investigate the contribution of feature reuse to the classification performance, we conducted various experiments on both AZS-II and one-shot tasks. Since the classifiers require the support sets [3], which means the adaptation still contributes to the classification performance, to separate the feature reuse from the adaptation, we resort to analyzing the clusterability of the features extracted by CNAP-CMF. The analysis shows that they have a much smaller inner-class distance than CNAPs-extracted features while maintaining a comparable inter-class distance (see detail in Section 4.2), indicating a better clusterability.

As a result, the feature adaptation can be stopped in CNAP-CMF, i.e., the adaptation parameters can be pre-computed and stored before the test stage to avoid repetitive computation. Then the stored adaptation parameters can be reused at the test stage. So the mean feature encoder and parameter adaptation networks are removed in the test stage, leading to the reduction of parameter amount by 40.48%. The main contributions are concluded as follows.

1. Motivated by ANIL, we show that the feature reuse is more important in

¹CMF is a lightweight module which can be embedded in the mean encoder of original CNAPs, called CNAP-CMF.

metric-based few-shot methods by experimenting with Almost Zero-Shot (AZS) tasks, AZS-I and AZS-II. In AZS-II tasks, the adaptation can be completely stopped, which only needs a randomly chosen support set from any arbitrary sub-dataset in the test stage.

2. CMF is proposed to address the problem of scattered mean embeddings yielded by CNAPs by mapping varying support sets to a canonical form. The canonical form means stable mean embeddings, enabling CNAP-CMF to outperform CNAPs by a large margin on AZS-II and one-shot tasks.
3. After CNAP-CMF is fully trained, the adaptation of the feature extractor is stopped. Naturally, the structures responsible for feature adaptation can be removed in the test stage, and only the frozen ResNet-18 and the stored adaptation network of linear classifiers need to be stored. This reduces the number of parameters by 40.48%.

The rest of the paper is organized as follows. Section 2 overviews the meta-learning and few-shot learning methods; Section 3 formulates CNAPs and CNPs [7] in a mathematical form, then presents the canonical mean filter (CMF); Section 4 presents the experimental results on multi-task classification, and conducts the ablation experiments to analyze the proposed CMF; and the conclusion is given in Section 5.

2. Related Works

Few-shot learning methods can be divided into metric-based methods and gradient-based methods. For metric-based methods, Authors [1] proposed the episode fashion for deep few-shot learning and designed the MatchingNets addressing few-shot tasks. Following [1], Snell *et al.* [8] proposed Prototypical Networks for Few-shot Learning, which used a KNN-like method to determine the unseen class of a test sample according to the feature distance between the test sample and each support sample.

For gradient-based methods, MAML [2] was proposed to yield adaptive gradients in inner loop for fast adaptation in test stage. Following [2], many variants

of MAML were designed. FOMAML [9] dropped the second-order item to avoid computing the Hessian matrix in MAML. Nichol *et al.* proposed Reptile [10] to address the problem of computing the complex Hessian matrix in MAML by an analytical first-order gradient. Wang *et al.* proposed Meta-Metric-Learner [11] to combine the advantages of both the metric-based and optimization-based methods for handling the varying number of classes, and hence generate more generalized metrics for classification across tasks.

Since Conditional Neural Processes [7] was proposed, the CNP-based methods proposed in [7, 12, 13, 14, 15] have become more and more popular because of their simplified computation of complex covariance matrix in KNN-based methods and their satisfying performance on 1-D and 2-D regression tasks. NPs [12] further added real random sample in CNPs and used the Reparameterization Trick proposed in Variational Autoencoder [16]. ANPs [13] incorporated the attention mechanism commonly used in the Natural Language Process (NLP), which includes the single-head and multi-head attention, to make the conditional inference of NP be more focused on the key information. ConvCNPs [14] make the CNPs capable of modeling translation equivariance, which is an important inductive bias for many learning problems, in the data. CNAPs [4] use a fully trained model to provide enough discrimination for the multi-task classification tasks, which improved the classification capability over the CNPs.

CNP-based methods explicitly employ an adaptation module to adapt the parameters of feature-extractor structure to the unseen test samples. The ANIL [3] however, thought that the universal feature representation played a more important role than the adaptation module for few-shot learning. Following the ANIL, we further designed two experiments, AZS-I and AZS-II, and the experimental results coincide with the point view of the ANIL. Observing this, this work designed an attention module to realize the canonical mean filter (CMF). The CMF provides a stable transfer feature that can guide the feature extractor to generate the universal feature representation.

Similar to Dynamic Convolution (DY) [17], the proposed CMF can be taken as a type of dynamic filters. But different from DY, the CMF aims to generate

sample-independent features that are stable across different tasks; DY aims to generate sample-dependent features for the classification task that are often (desired to be) significantly distinct across different classes.

3. Proposed method

This section presents the canonical mean filter (CMF) that is able to map varying support sets to a canonical form. To clearly state the rationale of CMF, we firstly need to mathematically formulate the CNAP-based methods. With the formulation, the mean shifting is analyzed and shown to be over-sensitive to the variation of support sets. Then, we propose CMF to alleviate the over-sensitiveness by mapping the input images to a canonical form, and provide a theoretical explanation from the Bayesian inference view.

3.1. Mathematical Formulation of CNAPs

CNAPs originate from CNPs. For the completeness, the CNPs [7] are briefly introduced here. Let \mathcal{X}^C and \mathcal{X}^T denote context image dataset and target image dataset, and \mathcal{Y}^C and \mathcal{Y}^T denote their labels.

CNPs use Neural Networks (NNs) to build the mean mapping parameterized by θ from the context image dataset to feature space, $F(\cdot, \theta) : \mathcal{X}^C \rightarrow \mathcal{R}^C$. $\mathcal{R}^C = F(\mathcal{X}^C, \theta)$ encodes the distribution information of support sets $\{\mathcal{X}^C, \mathcal{Y}^C\}$ and is used to generate the adaptation parameter ϕ for the inference model by

$$\pi(\cdot, \mathcal{R}^C) : \varphi \rightarrow \phi,$$

where φ represents the original parameter of the inference model to be adapted. We call the parameter adaptation *mean shifting* in this work. Then, the inference model $G(\phi, \cdot)$ predicts the classes of the target set \mathcal{X}^T by

$$\mathcal{Y}_{pred}^T = G(\phi, \mathcal{X}^T) = G\left(\pi(\varphi, F(\mathcal{X}^C, \theta)), \mathcal{X}^T\right). \quad (1)$$

In the training process, CNPs optimize G jointly over θ and φ in Equation 1 by maximizing the likelihood given $(\mathcal{X}^T, \mathcal{Y}^T)$. Formally,

$$\hat{\theta}, \hat{\varphi} = \arg \max_{\theta, \varphi} p(\mathcal{Y}^T | G(\pi(\varphi, F(\mathcal{X}^C, \theta)), \mathcal{X}^T)). \quad (2)$$

CNAPs [4] build a simple convolutional neural network to get \mathcal{R}^C , then use a mean operator to aggregate the features over all samples to get the mean vector \mathcal{R}_m^C ,

$$\mathcal{R}_m^C = \frac{1}{S} \sum_{i=1}^S \mathcal{R}_i^C,$$

where S is the cardinality of the input support sets.

Following the FiLM layers [18], CNAPs design an adaptation network parameterized by $\gamma = \{\gamma_w, \gamma_b\}$ to realize the mapping π in Eq. 1. Formally,

$$\phi = \pi(\varphi, \gamma, \mathcal{R}_m^C) = (\gamma_w \otimes \mathcal{R}_m^C) \times \varphi + (\gamma_b \otimes \mathcal{R}_m^C), \quad (3)$$

where \otimes represents the convolution operation.

To build a powerful feature extractor for the inference model, CNAPs use the ResNet-18 [19] with every convolutional layer being followed by FiLM layers [18]. The ResNet-18 is fully trained on ImageNet-1K and outputs 512-D embeddings for the final linear classification. After being trained on ImageNet-1K, the parameters φ of the ResNet18 are frozen, i.e., they will not be updated in the subsequent training process of CNAPs. $\pi(\varphi, \gamma, \mathcal{R}_m^C)$ adapts φ of the frozen fully-trained ResNet-18 model to a new target dataset according to \mathcal{R}_m^C and γ . With π , the maximum likelihood in Equation 2 will be cast as

$$\hat{\theta}, \hat{\gamma} = \arg \max_{\theta, \gamma} p(\mathcal{Y}^T | G(\pi(\varphi, \gamma, F(\mathcal{X}^C, \theta)), \mathcal{X}^T)). \quad (4)$$

In Eq. 4, CNAPs optimize $G(\phi, \mathcal{X}^T)$ jointly over θ and γ . Since γ will also be driven by \mathcal{R}_m^C , i.e., its update depends on \mathcal{R}_m^C , the over-sensitivity comes from $F(\cdot, \theta)$. Thus, to alleviate the over-sensitivity of CNAPs to the varying support sets, a critical step is to design $F(\cdot, \theta)$ such that $\mathcal{R}_m^C = F(\mathcal{X}^C, \theta)$ does not change dramatically with \mathcal{X}^C . Motivated by this observation, this work proposes the canonical mean filter that generate stable features for the adaptation to realize the *mean shifting*.

3.2. Canonical Mean Filter

To strengthen the stability of $\mathcal{R}_m^C = F(\mathcal{X}_C, \theta)$, this work proposed Canonical Mean Filter (CMF). CMF maps different samples to a canonical form, reducing

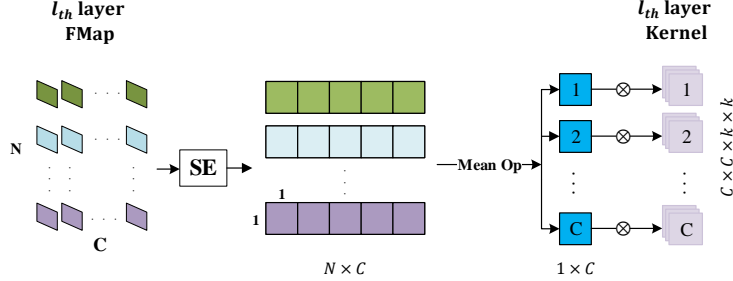


Figure 2: **Canonical Mean Filter architecture.** To build stable mean shifting, the salient features of each support sample in the $(l-1)$ -th layer are extracted by Squeeze-and-Excitation module, and then are averaged across all samples to get the canonical mapping weights for the kernels in the l -th layer.

the over-sensitivity of CNAPs to the wide variation of support sets, and even helping remove the demand on the support sets. Note, it is important that \mathcal{R}_m^C represents the mean vector for adaptation on the whole dataset rather than only on a particular task. This hence means that θ is desired to be optimized by the marginal likelihood of all tasks instead of particular tasks. In fact, task-specific likelihood is more difficult to be optimized than marginal likelihood of all tasks in few-shot tasks; and the former gives an inferior performance to the latter [20, 21].

Seeing this, we design CMF to realize the marginal likelihood optimization over all tasks by a kernel way to get representative and stable \mathcal{R}_m^C . As is shown in Fig. 2, a designed attention module is used to extract the most salient feature $\mathcal{S}\mathcal{F}^{l-1} \in R^{N \times C}$ of each sample at the $(l-1)$ -th layer, and then $\mathcal{S}\mathcal{F}^{l-1}$ are averaged across all samples for fusing features by

$$\overline{\mathcal{S}\mathcal{F}^{l-1}} = \frac{1}{N} \sum_0^{N-1} \mathcal{S}\mathcal{F}^{l-1}, \quad (5)$$

where N is the number of samples in a task. $\overline{\mathcal{S}\mathcal{F}^{l-1}}$ in Eq. 5 serving as the weights, are assigned to the kernels in the l -th layer. Tab. 1 gives the structure the designed attention module.

Table 1: The architecture of the proposed CMF

operators	kernel shape	output shape
Input	\mathcal{F}^{l-1}	$N \times C \times W \times H$
Pooling	Max Pooling	$N \times C$
FC1	$C \times \frac{C}{4}$	$N \times \frac{C}{4}$
ReLU	-	-
FC2	$\frac{C}{4} \times C$	$N \times C$
Output	$\mathcal{S}\mathcal{F}^{l-1}$	$N \times C$

For explaining the CMF, we follow CNAPs and assume that all convolutional layers in $F(\cdot, \theta)$ contain the same number of kernels, and thus the output channel numbers are also same. Let \mathcal{F}^l denote the l_{th} layer, $l \in \{1, \dots, L\}$, and \mathcal{K}^l denote the set of kernels in \mathcal{F}^l . CMF can be formulated as

$$\begin{aligned} \mathcal{F}^l &= (\overline{\mathcal{S}\mathcal{F}^{l-1}} \cdot \mathcal{K}^l) \otimes \mathcal{F}^{l-1} \\ &= \overline{\mathcal{S}\mathcal{F}^{l-1}} \cdot (\mathcal{K}^l \otimes \mathcal{F}^{l-1}). \end{aligned} \quad (6)$$

In Eq. 6, $\overline{\mathcal{S}\mathcal{F}^{l-1}}$ containing the average information of all samples will undermine the (biased) influence of individual samples on \mathcal{F}^l . Like Dynamic Filter technology, the mean weights $\overline{\mathcal{S}\mathcal{F}^{l-1}}$ assigned to the kernels in \mathcal{F}^l will bring the model adaptability to unseen data [22]. In addition, the averaging and fusion are carried out at every convolutional layer in this work rather than only at the final layer, which makes the fusion more effective in hierarchical architectures [21] and hence the ideal mean embedding of $F(\mathcal{X}^C, \theta)$ more accessible.

3.3. Bayesian View of CMF

This section analyzes the CMF and CNAPs from Bayesian inference view. At the training stage, the mean encoder of the CNAPs were trained to maximize the classification accuracy within a particular task. This amounts to searching for the mean vector \mathcal{R}_m^C that maximizes the likelihood of $p(\mathcal{Y}_k^T | \mathcal{X}_k^T, \mathcal{R}_m^C)$.

Formally,

$$\hat{\theta} = \arg \max_{\theta} p(\mathcal{Y}_k^T | \mathcal{X}_k^T, F(\mathcal{X}_k^C, \theta)), \quad (7)$$

where $\mathcal{R}_m^C = F(\mathcal{X}_k^C, \theta)$ and the support sets \mathcal{X}_k^C are chosen from the task.

The obtained $\hat{\theta}$ by Eq. (7) is task-specific, and $F(\mathcal{X}_k^C, \hat{\theta})$ is expected to be able to yield a task-specific feature \mathcal{R}_m^C that provides a good prior for parameter adaptation within the task. Unfortunately, the task-level optimization for θ does not perform satisfactorily on few-shot tasks [20, 23], since $F(\mathcal{X}_j^C, \hat{\theta})$ will not provide a good prior for an unseen task.

As a comparison, CMF can be formulated as a kernel method of searching the Bayesian parameter θ that maximizes the marginal likelihood over all K tasks. Formally,

$$\begin{aligned} \hat{\theta} &= \arg \max_{\theta} \prod_{k=1}^K p(\mathcal{Y}_k^T | \mathcal{X}_k^T, F(\mathcal{X}_k^C, \theta)) \\ &= \arg \max_{\theta} \int \prod_{k=1}^K p(\mathcal{Y}_k^T | \mathcal{X}_k^T, F(\mathcal{X}_k^C, \theta)) p(\mathcal{X}_k^C) d\mathcal{X}_k^C \\ &= \arg \max_{\theta} \frac{1}{K} \int \prod_{k=1}^K p(\mathcal{Y}_k^T | \mathcal{X}_k^T, F(\mathcal{X}_k^C, \theta)) d\mathcal{X}_k^C. \end{aligned} \quad (8)$$

where $p(\mathcal{X}_k^C)$ always equals to $\frac{1}{K}$, and $\{\mathcal{Y}_k^T, \mathcal{X}_k^T\}, k = 1, \dots, K$, denotes the target set for the k_{th} task. Once $\hat{\theta}$ is obtained from Eq. (8), $\hat{\mathcal{R}}_m^C = F(\mathcal{X}^C, \hat{\theta})$ with any arbitrary \mathcal{X}^C can provide the best average classification performance on all tasks since the influence of \mathcal{X}^C on $\hat{\mathcal{R}}_m^C$ is significantly suppressed.

Patacchiola *et al.* proposed Deep Kernel Transfer (DKT) [20] to approximate the kernel parameterized by θ with the kernel of the Gaussian Process (GP) in Eq. 8 and realized the marginal optimization. However, GP kernels cannot approximate many generally unknown kernels, which leads to a bad fitting model. Although many kernels are generally unknown, we can use the output of the dynamic kernels to approximate the output of the unknown kernels. The CMF designs a canonical filter to yield a stable mean prior, approximating the prior generated by the $\hat{\theta}$ resulting from the marginal optimization over all support sets in Eq. (8).

4. Experiments

In this section, CNAP-CMF is compared with the state-of-the-art CNAPs for multi-task classification tasks on Meta-Datasets. Three tasks are designed in Section 4.1 to investigate the role of feature reuse: AZS-I, AZS-II, and one-shot tasks. Similar to CNAPs, the models are fully trained on two different training datasets, 1) all sub-datasets of Meta-Datasets, and 2) ImageNet-1K. The trained models are then tested on all sub-datasets of Meta-Datasets as well as MNIST, CIFAR-10, and CIFAR-100, in order to evaluate the cross-domain performance. Then the clustering performance of CNAPs and CNAP-CMF are analyzed in Section 4.2 to investigate the linear separability.

4.1. Multi-task Classification

This section reports the evaluation results of AZS-II and one-shot tasks on the whole test dataset of Meta-Dataset when the models are trained on Meta-Dataset. Also, the evaluated results of CNAPs (AR) and CNAP-CMF (AR) for one-shot tasks, whose models are fully trained on ImageNet-1k, are also reported. The result of AZS-I is reported in Table A.7.

4.1.1. Training Strategy

We follow the training strategy in CANPs [4], and only 2 NVIDIA Ti-1080 GPUs with 12G memory are used. Due to the limit of computation resource, the auto-regressive (AR) proposed in CNAPs is not used when the model is trained on Meta-Dataset, but used when the model is trained on ImageNet-1K.

All models are trained for 110,000 episodes with the Adam [24] optimizer. The learning rate is 0.0005 and the batch size is 16. The trained model is validated per 200 episodes during the training process. For the multi-dataset classification task, a model is considered to perform better than current model if it yields higher classification accuracy on over half of all sub-datasets.

4.1.2. Training on Meta-Dataset

Tab. 2 gives the classification performance of CNAP-CMF on AZS-II tasks. On Omniglot dataset, AZS-II, CNAP-CMF outperforms CNAPs 37.2%. Simi-

larly, for AZS-II, CNAP-CMF outperforms CNAPs by 38.3%, 20.7%, and 10.4% on Aircraft, Quick Draw, and MNIST datasets respectively. When CNAPs are directly applied to AZS-II tasks, where the fixed support set is randomly chosen in ImageNet-1k sub-dataset, the classification performance decreases significantly on Omniglot [6], Aircraft [25], Quick Draw, and MNIST. When the fixed support set is chosen in other sub-datasets, Table C.8 gives severer performance drop on all evaluated sub-datasets. CNAP-CMF on AZS-II tasks performs only slightly inferior to CNAPs on one-shot tasks.

Table 2: Multi-task image classification results. CNAPs and CNAP-CMF are tested on AZS-II and one-shot tasks respectively.

Datasets	CNAP	CNAP	CMF	CMF
	OneShot	AZS-II	OneShot	AZS-II
ImageNet	51.3	50.8	51.6	51.2
Omniglot	88	50.2	87.7	87.4
Aircraft	76.8	39.1	77.9	77.4
Birds	71.4	69.3	71.6	69.9
Textures	62.5	64	63.9	63.7
Quick Draw	71.9	49.8	71.6	70.5
Fungi	46	40.4	45.4	43.4
VGG Flower	89.2	80.5	89.7	89.4
Traffic Sign	60.1	59.1	61.3	61.4
MSCOCO	42	41.9	44.1	43
MNIST	88.6	78.7	89.2	89.1
CIFAR10	60	58.7	66.1	66.3
CIFAR100	48.1	47.6	50	51.3

For one-shot tasks, CNAP-CMF also outperforms CNAPs by 0.3% \sim 6% on most test sub-datasets. The reason is that different support sets in the same task can yield classification performance fluctuation due to unstable mean embeddings. To simply see the fluctuation, four support sets are randomly chosen from Omniglot dataset in the same task, and Table 3 gives the classification results. For example, on Task 3, the support set \mathcal{X}_1^S gives 76.5% classification accuracy, but \mathcal{X}_4^S gives 92%, 15.5% higher than \mathcal{X}_1^S . As a comparison, CMF addresses the inner-task performance fluctuation by generating stable mean embeddings which are almost independent of the support sets in a particular task.

Table 3: Classification result of CNAPs using different support sets for the same task on Omniglot. Unit: %.

Task	\mathcal{X}_1^S	\mathcal{X}_2^S	\mathcal{X}_3^S	\mathcal{X}_4^S
T1	93.5	88.9	91.5	90.1
T2	81.0	90.0	85.0	85.5
T3	76.5	80.0	79.5	92.0

4.1.3. Training on Single Dataset

Due to the limit of computation resource, the proposed AR in CNAPs that needs to be trained on the whole Meta-Dataset is not used in the following evaluation experiments. For verifying the effectiveness of the proposed CMF and maintaining the thoroughness of the whole evaluation experiments, AR is used in the following comparison experiments, in which the models are only trained on ImageNet sub-dataset.

As is given in Tab. 4, CNAP-CMF (AR) outperforms CNAPs (AR) on almost all sub-datasets of Meta-Datasets. Although the model is only trained on ImageNet-1K, the pre-trained ResNet-18 model brings the inference enough separability capability to make the CNAPs (AR) can be generalized to other datasets. Also, CMF making the mean mapping $F(\cdot, \theta)$ learn a better mean representation when the unseen data is input. The better representation allows the inference model $G(\phi, \mathcal{X}^T)$ to be adapted to the target distributions more correctly.

4.2. Clustering Analysis of Extracted Features in AZS Style

Similar to the reasons described in the ANIL, the adaptation part cannot be removed in the classifiers. This means that the corresponding support sets cannot be removed in the classifiers of CNAPs. Seeing this, the clustering performance of features, which are extracted by the feature extractors without adaptation, is analyzed in this section. The PCA is used to visualize the extracted features for showing the better linear separability of CNAP-CMF features.

Table 4: Classification results of CNAPs-One (AR), CNAP-CMF-One (AR) and other SOTA methods are compared. The evaluated models are trained on ImageNet-1K only, and evaluated on the whole Meta-Dataset.

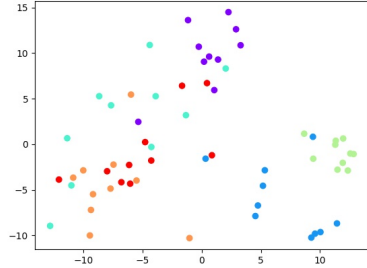
Datasets	ProtoNet	MatchingNet	CNAP	CMF
	One (AR)	One (AR)	One (AR)	One (AR)
ImageNet	50.5	45.0	50.6	50.9
Omniglot	60.0	52.3	45.2	45.7
Aircraft	53.1	49.0	36.0	37.2
Birds	68.8	62.2	60.7	61.2
Textures	66.6	64.2	67.5	67.4
Quick Draw	49.0	42.9	42.3	42.9
Fungi	39.7	34.0	30.1	31.3
VGG Flower	85.3	80.1	70.7	71.0
Traffic Sign	47.1	47.8	53.3	53.1
MSCOCO	41.0	35.0	45.2	45.6
MNIST			70.4	72.3
CIFAR10			65.2	66.7
CIFAR100			53.6	54.3

The example figures shown in the right column of Fig. 3 are the 512-D features extracted by CNAPs in AZS style, which are linear inseparable, especially the features of Texture sub-dataset. As a comparison, the features extracted by CNAP-CMF form obvious separable clusters, which are shown in the right column and indicate the more powerful feature extractor.

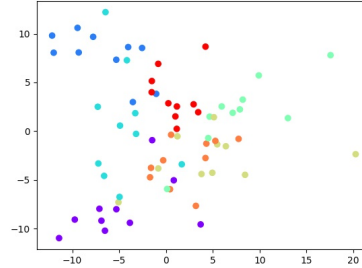
Table 5: The clusterable property comparison is analyzed by inner-class and inter-class Mahalanobis distance of the extracted features between CNAPs and CNAP-CMF for AZS tasks.

Datasets	CNAPs		CNAP-CMF	
	Inner-class dist	Inter-class dist	Inner-class dist	Inter-class dist
Omniglot	6.57	12.74	2.25	11.91
Aircraft	4.78	9.23	1.51	8.73
Texture	5.62	10.54	1.73	9.19
QucikDraw	5.64	10.92	1.78	10.18

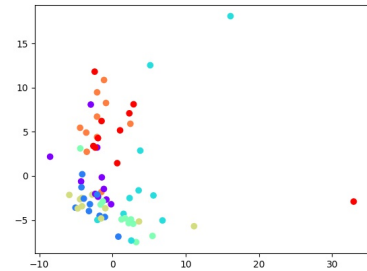
For quantitative analysis, the inner-class and inter-class Mahalanobis distance between the extracted features are also given in Table 5. Firstly, PCA is used to reduce the dimensionality of the original 512-D feature embedding



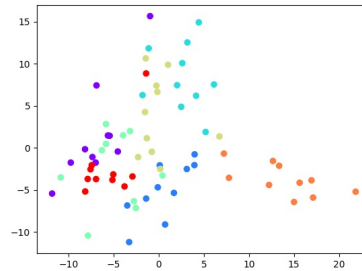
(a) QuickDraw with CNAPs



(b) QuickDraw with CNAP-CMF



(c) Textures with CNAPs



(d) Textures with CNAP-CMF

Figure 3: The clusterable property analyses of the extracted features with CNAPs and CMFs on QuickDraw and Textures datasets. The fixed support sets are randomly selected in ImageNet-1K.

to 64-D for reducing the effect of unimportant features because Mahalanobis distance is more sensitive to the noised features than Euclidean distance. The Mahalanobis distance is used because it can reflect the distance along the data distribution [26].

As given in Table 5, for example, on Omniglot, the inner-class distance of CNAP-CMF is 2.25, and the corresponding inner-class distance of CNAPs is 6.57. Simultaneously, the inter-class distance of CNAP-CMF is 11.91, while the corresponding inter-class distance of CNAPs is 12.74. Obviously, the much smaller inner-class distance and similar inter-class make the extracted features, without adaptation, of CNAP-CMF more linear separable than CNAPs. Simi-

larly, the clustering quantitative analysis on Aircraft, Texture, and QucikDraw also verifies the effectiveness of CNAP-CMF.

4.3. Parameter Reduction and Inference Acceleration at The Test Stage

The mean prior \mathcal{R}_m^C generated by the mean encoder of CNAP-CMF is stable, and can be computed with any arbitrary support set. Thus, the mean prior \mathcal{R}_m^C and the vectors for parameter shifting, $(\gamma_w \otimes \mathcal{R}_m^C)$ and $(\gamma_b \otimes \mathcal{R}_m^C)$, can be pre-computed in Eq. 3. Consequently, the two sub-networks, the mean encoder and the adaptation network, can be removed, which hence allows for the inference to be accelerated. The two sub-networks account for about 40% parameter amount. For each sub-dataset of Meta-Dataset, the running time of CNAPs and CNAP-CMF for the sampled 600 tasks is computed. Table 6 gives the parameter amount and inference time. The parameter amount of CNAPs is reduced from 21.3M to 12.7M, and the inference time is reduced from $(3.5 + 20.7 + 12.3)$ s to 12.3s.

Table 6: The parameter amount and the average running time for 600 tasks (for each sub-dataset) over all sub-datasets of Meta-Dataset.

	# Param (M)	Encoder (s)	Adaptation (s)	ResNet (s)
CNAPs	21.3	3.5	20.7	12.3
CNAP-CMF	12.7	0.0	0.0	12.3

5. Conclusion

This paper investigated the role of feature reuse and the adaptation in the metric-based few-shot method, CNAPs. We designed two Almost Zero-Shot (AZS) experiments, AZS-I and AZS-II. In AZS-I, a support set is randomly chosen from each sub-dataset and used on all tasks within it; in AZS-II, a support set is randomly chosen from a sub-dataset but used on all tasks of all sub-dataset. Both AZS-I and AZS-II showed that the support sets were not necessary and the performance decrease of CNAPs without the adaptation

originates from the over-sensitiveness of the mean embeddings to the variation of support sets. To deal with the over-sensitiveness, we proposed a Canonical Mean Filter that can map varying support sets to a canonical form. The CMF can allow for the adaptation to be stopped in CNAPs without the performance drop, and the stopped adaptation leads to 40.48% parameter reduction in the test stage. The analysis on the clustering property of extracted features by CNAP-CMF showed that they were more separable than the features extracted by CNAPs, verifying that the feature reuse was more important.

References

- [1] O. Vinyals, C. Blundell, T. Lillicrap, k. kavukcuoglu, D. Wierstra, Matching networks for one shot learning, in: D. Lee, M. Sugiyama, U. Luxburg, I. Guyon, R. Garnett (Eds.), *Advances in Neural Information Processing Systems*, Vol. 29, Curran Associates, Inc., 2016.
URL <https://proceedings.neurips.cc/paper/2016/file/90e1357833654983612fb05e3ec9148c-Paper.pdf>
- [2] C. Finn, P. Abbeel, S. Levine, Model-Agnostic Meta-Learning for Fast Adaptation of Deep Networks, 2017.
URL <http://arxiv.org/abs/1703.03400>
- [3] A. Raghu, M. Raghu, S. Bengio, O. Vinyals, Rapid learning or feature reuse? towards understanding the effectiveness of maml, in: *International Conference on Learning Representations*, 2020.
URL <https://openreview.net/forum?id=rkgMkCEtPB>
- [4] J. Requeima, J. Gordon, J. Bronskill, S. Nowozin, R. E. Turner, Fast and flexible multi-task classification using conditional neural adaptive processes, in: H. Wallach, H. Larochelle, A. Beygelzimer, F. d'Álché-Buc, E. Fox, R. Garnett (Eds.), *Advances in Neural Information Processing Systems 32*, Curran Associates, Inc., 2019, pp. 7957–7968.

- [5] E. Triantafillou, T. Zhu, V. Dumoulin, P. Lamblin, U. Evci, K. Xu, R. Goroshin, C. Gelada, K. Swersky, P.-A. Manzagol, H. Larochelle, Meta-dataset: A dataset of datasets for learning to learn from few examples, in: International Conference on Learning Representations, 2020.
- [6] B. M. Lake, R. Salakhutdinov, J. B. Tenenbaum, Human-level concept learning through probabilistic program induction, *Science* 350 (6266) (2015) 1332–1338. arXiv:<https://science.sciencemag.org/content/350/6266/1332.full.pdf>, doi:10.1126/science.aab3050.
URL <https://science.sciencemag.org/content/350/6266/1332>
- [7] G. M, R. D, M. CJ, R. T, S. D, S. M, T. YW, R. DJ, EslamiSM, Conditional neural processes, in: International Conference on Machine Learning, 2018.
- [8] J. Snell, K. Swersky, R. Zemel, Prototypical networks for few-shot learning, in: I. Guyon, U. V. Luxburg, S. Bengio, H. Wallach, R. Fergus, S. Vishwanathan, R. Garnett (Eds.), *Advances in Neural Information Processing Systems*, Vol. 30, Curran Associates, Inc., 2017.
URL <https://proceedings.neurips.cc/paper/2017/file/cb8da6767461f2812ae4290eac7cbc42-Paper.pdf>
- [9] A. Biswas, S. Agrawal, First-order meta-learned initialization for faster adaptation in deep reinforcement learning, 2018.
- [10] A. Nichol, J. Achiam, J. Schulman, On first-order meta-learning algorithms, ArXiv abs/1803.02999.
- [11] D. Wang, Y. Cheng, M. Yu, X. Guo, T. Zhang, A hybrid approach with optimization-based and metric-based meta-learner for few-shot learning, *Neurocomputing* 349 (2019) 202–211. doi:<https://doi.org/10.1016/j.neucom.2019.03.085>.
URL <https://www.sciencedirect.com/science/article/pii/S0925231219305363>

- [12] M. Garnelo, J. Schwarz, D. Rosenbaum, F. Viola, D. J. Rezende, S. Eslami, Y. W. Teh, Neural processes, arXiv preprint arXiv:1807.01622.
- [13] H. Kim, A. Mnih, J. Schwarz, M. Garnelo, A. Eslami, D. Rosenbaum, O. Vinyals, Y. W. Teh, Attentive neural processes, arXiv preprint arXiv:1901.05761.
- [14] J. Gordon, W. P. Bruinsma, A. Y. Foong, J. Requeima, Y. Dubois, R. E. Turner, Convolutional conditional neural processes, arXiv preprint arXiv:1910.13556.
- [15] A. Y. Foong, W. P. Bruinsma, J. Gordon, Y. Dubois, J. Requeima, R. E. Turner, Meta-learning stationary stochastic process prediction with convolutional neural processes, arXiv preprint arXiv:2007.01332.
- [16] D. P. Kingma, M. Welling, Auto-encoding variational bayes, arXiv preprint arXiv:1312.6114.
- [17] Y. Chen, X. Dai, M. Liu, D. Chen, L. Yuan, Z. Liu, Dynamic convolution: Attention over convolution kernels, in: Proceedings of the IEEE Conference on Computer Vision and Pattern Recognition, 2020.
URL <http://arxiv.org/abs/1912.03458>
- [18] E. Perez, F. Strub, H. de Vries, V. Dumoulin, A. C. Courville, Film: Visual reasoning with a general conditioning layer, in: AAAI, 2018.
- [19] K. He, X. Zhang, S. Ren, et al., Deep residual learning for image recognition, in: IEEE Conference on Computer Vision and Pattern Recognition, 2015, pp. 770–778.
- [20] M. Patacchiola, J. Turner, E. J. Crowley, A. Storkey, Bayesian meta-learning for the few-shot setting via deep kernels, in: Advances in Neural Information Processing Systems, 2020.
- [21] H. Robbins, AN EMPIRICAL BAYES APPROACH TO STATISTICS, University of California Press, 2020, pp. 157–164. doi:doi:10.1525/

9780520313880-015.

URL <https://doi.org/10.1525/9780520313880-015>

- [22] Y. Chen, X. Dai, M. Liu, D. Chen, Z. Liu, Dynamic convolution: Attention over convolution kernels, in: 2020 IEEE/CVF Conference on Computer Vision and Pattern Recognition (CVPR), 2020.
- [23] Y. Liu, B. Schiele, Q. Sun, An ensemble of epoch-wise empirical bayes for few-shot learning, in: European Conference on Computer Vision (ECCV), 2020.
- [24] D. P. Kingma, J. Ba, Adam: A method for stochastic optimization, in: Y. Bengio, Y. LeCun (Eds.), 3rd International Conference on Learning Representations, ICLR 2015, San Diego, CA, USA, May 7-9, 2015, Conference Track Proceedings, 2015.
URL <http://arxiv.org/abs/1412.6980>
- [25] S. Maji, J. Kannala, E. Rahtu, M. Blaschko, A. Vedaldi, Fine-grained visual classification of aircraft, Tech. rep. (2013). [arXiv:1306.5151](https://arxiv.org/abs/1306.5151).
- [26] P. Bateni, R. Goyal, V. Masrani, F. Wood, L. Sigal, Improved few-shot visual classification, in: Proceedings of the IEEE/CVF Conference on Computer Vision and Pattern Recognition (CVPR), 2020.

Appendix A. AZS-I Experiments

Table A.7: Multi-task image classification results. CNAPs and CNAP-CMF are tested on AZS-I and one-shot tasks: CNAPs-One, CNAPs-AZS, and CNAP-CMF-AZS-I.

Datasets	CNAP-One	CNAP-AZS-I	CMF-AZS-I
ImageNet	51.3	50.9	51.2
Omniglot	88	87.2	87.6
Aircraft	76.8	75.9	77.2
Birds	71.4	70.2	71.4
Textures	62.5	63.1	63.0
Quick Draw	71.9	71.5	70.5
Fungi	46	45.4	43.3
VGG Flower	89.2	87.3	89.6
Traffic Sign	60.1	58.5	62.0
MSCOCO	42	41.7	43.4
MNIST	88.6	87.1	89.1
CIFAR10	60	58.7	65.3
CIFAR100	48.1	47.6	50.9

Appendix B. Some Clustering Visualization

Appendix C. Different Support Sets Selection Comparison

Actually, for AZS-II, the unstable CNAPs perform more poor than the fixed support sets are selected from ImageNet. As shown in Table C.8, the sub-datasets in the first row mean when the fixed support sets are selected in the corresponding sub-dataset. The column under the sub-datasets gives the corresponding evaluated performance. Obviously, except the performance in bold, which means the evaluated performance on the test sub-dataset when the support sets are selected from the corresponding sub-dataset, the evaluated performance drops a lot on other sub-datasets.

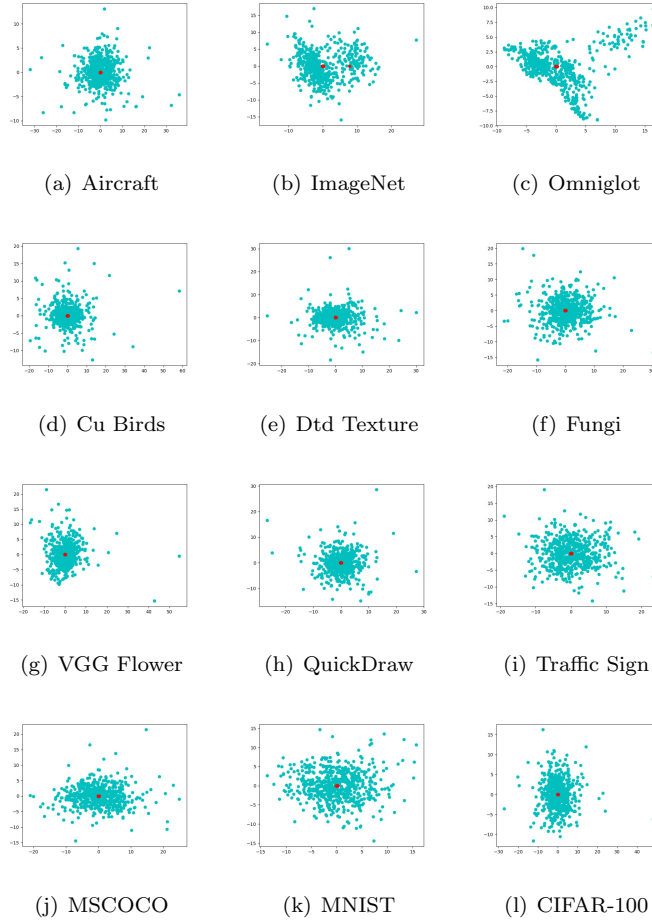
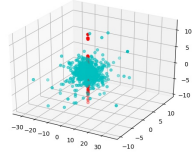
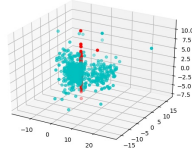


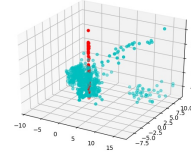
Figure B.4: Clustering Visualization of \mathcal{R}_i^T (where $i \in \{1, 2, \dots, N\}$, and N is the number of test image datasets in Meta-Datasets) with the model trained on Meta-Datasets. Two dimensionality principal components are extracted by PCA.



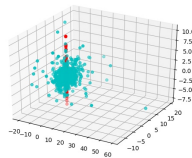
(a) Aircraft



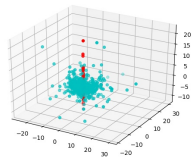
(b) ImageNet



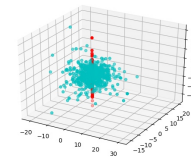
(c) Omniglot



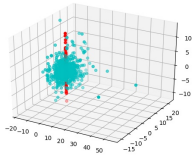
(d) Cu Birds



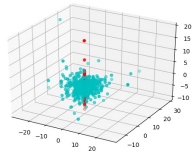
(e) Dtd Texture



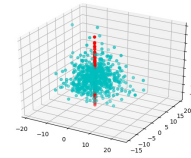
(f) Fungi



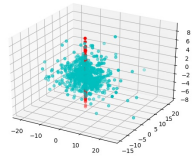
(g) VGG Flower



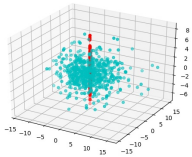
(h) QuickDraw



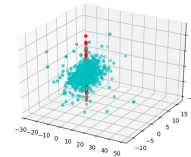
(i) Traffic Sign



(j) MSCOCO



(k) MNIST



(l) CIFAR-100

Figure B.5: Clustering Visualization of \mathcal{R}_i^T (where $i \in \{1, 2, \dots, N\}$, and N is the number of test image datasets in Meta-Datasets) with the model trained on Meta-Datasets. Three dimensionality principal components are extracted by PCA.

Table C.8: The performance of CNAPs-AZS-II is evaluated on Meta-Datasets when the fixed support sets are selected from the sub-datasets except ImageNet.

Datasets	Omniglot	Aircraft	Birds	Textures	Quick Draw	Fungi	VGG Flower	Traffic Sign	MSCOCO	MNIST	CIFAR10	CIFAR100
CNAPs-AZS-II												
ImageNet	31.0	38.7	45.5	43.0	42.1	50.1	46.5	50.1	50.9	33.2	51.3	50.8
Omniglot	85.1	67.6	55.6	55.4	78.5	57.7	65.9	60.0	56.1	84.2	55.3	52.5
Aircraft	51.6	74.6	55.5	54.7	67.2	59.3	68.9	55.2	44.7	53.3	37.2	36.2
Birds	29.1	51.1	67.6	66.7	53.9	67.9	62.3	69.9	69.8	33.4	67.7	65.8
Textures	49.9	56.7	58.4	55.6	56.0	63.8	60.8	64.6	65.7	50.6	64.9	64.4
Quick Draw	60.4	60.9	46.3	44.8	70.6	54.5	61.4	57.9	51.7	63.5	51.9	50.8
Fungi	19.0	30.9	39.6	35.8	34.0	42.7	41.1	42.5	41.2	21.8	38.2	37.6
VGG Flower	63.7	73.6	74.5	70.5	82.7	81.8	83.2	83.4	80.8	70.7	79.6	78.7
Traffic Sign	56.9	47.4	48.4	47.7	53.6	49.7	53.7	53.0	54.5	56.4	56.8	58.0
MSCOCO	29.5	34.0	39.5	36.7	38.3	43.6	40.9	47.5	47.1	32.1	47.5	47.7
MNIST	90.6	86.4	74.9	74.6	87.9	76.2	83.6	78.2	78.6	90.5	79.2	79.3
CIFAR10	45.2	50.7	53.7	52.1	56.6	59.0	54.2	62.2	65.8	51.1	67.8	67.0
CIFAR100	29.8	33.4	38.1	34.3	40.0	44.0	40.1	49.7	52.2	32.5	53.4	54.1
CNAP-CMF-AZS-II												
ImageNet	50.8	51.5	51.0	50.6	50.7	50.6	51.4	50.4	50.5	51.2	50.4	50.5
Omniglot	88.0	86.8	87.8	88.0	88.2	88.5	88.0	87.6	88.0	87.6	87.9	87.9
Aircraft	73.4	76.6	73.6	72.9	73.1	73.0	73.0	73.1	73.7	73.4	74.2	73.1
Birds	69.2	69.6	71.3	70.0	70.4	69.9	69.9	70.1	69.1	70.6	70.2	70.0
Textures	59.1	60.8	59.7	62.9	59.3	60.0	60.0	59.8	59.6	60.2	59.9	59.5
Quick Draw	70.4	70.0	69.7	70.1	70.6	70.4	69.5	70.0	69.7	70.3	70.7	69.9
Fungi	43.4	43.4	43.4	42.1	43.6	44.2	43.6	43.8	44.3	43.5	43.0	44.1
VGG Flower	87.5	87.9	87.9	88.5	87.5	87.9	88.2	88.0	87.3	88.4	88.1	88.1
Traffic Sign	60.0	61.8	61.1	60.1	60.2	61.5	60.7	62.1	61.2	61.6	61.7	61.4
MSCOCO	45.4	43.9	45.5	44.0	45.3	44.7	44.4	45.6	46.9	44.4	44.2	44.1
MNIST	89.0	88.1	88.9	88.5	88.5	88.9	88.5	88.5	88.9	89.5	89.2	88.8
CIFAR10	62.5	62.7	62.7	62.6	62.5	62.9	63.2	62.2	62.8	63.6	63.8	63.6
CIFAR100	49.7	48.8	49.4	47.1	47.8	47.5	48.3	47.9	47.7	48.1	47.8	49.3